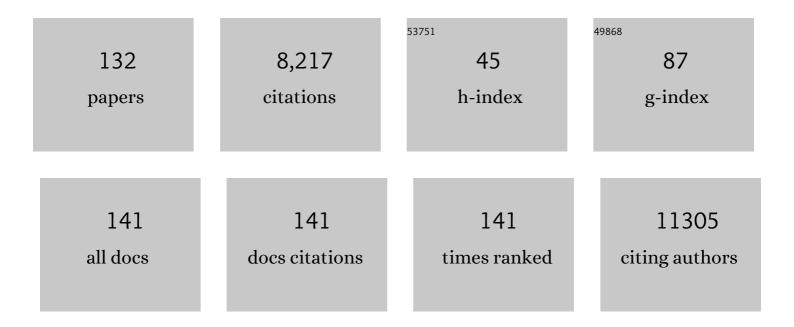
Zhigang Zhao

List of Publications by Year in descending order

Source: https://exaly.com/author-pdf/6858800/publications.pdf Version: 2024-02-01



#	Article	IF	CITATIONS
1	Noble metal-comparable SERS enhancement from semiconducting metal oxides by making oxygen vacancies. Nature Communications, 2015, 6, 7800.	5.8	534
2	Nanoporousâ€Walled Tungsten Oxide Nanotubes as Highly Active Visibleâ€Lightâ€Driven Photocatalysts. Angewandte Chemie - International Edition, 2008, 47, 7051-7055.	7.2	383
3	Singleâ€Crystalline Tungsten Oxide Quantum Dots for Fast Pseudocapacitor and Electrochromic Applications. Advanced Materials, 2014, 26, 4260-4267.	11.1	350
4	Semiconductor SERS enhancement enabled by oxygen incorporation. Nature Communications, 2017, 8, 1993.	5.8	306
5	Synergy of W ₁₈ O ₄₉ and Polyaniline for Smart Supercapacitor Electrode Integrated with Energy Level Indicating Functionality. Nano Letters, 2014, 14, 2150-2156.	4.5	275
6	Coupling Molecularly Ultrathin Sheets of NiFe-Layered Double Hydroxide on NiCo ₂ O ₄ Nanowire Arrays for Highly Efficient Overall Water-Splitting Activity. ACS Applied Materials & Interfaces, 2017, 9, 1488-1495.	4.0	244
7	Graphene-based materials for capacitive deionization. Journal of Materials Chemistry A, 2017, 5, 13907-13943.	5.2	242
8	Fusing electrochromic technology with other advanced technologies: A new roadmap for future development. Materials Science and Engineering Reports, 2020, 140, 100524.	14.8	227
9	Tungsten Oxide Materials for Optoelectronic Applications. Advanced Materials, 2016, 28, 10518-10528.	11.1	222
10	Composite anode material of silicon/graphite/carbon nanotubes for Li-ion batteries. Electrochimica Acta, 2006, 51, 4994-5000.	2.6	207
11	Metal–Organic Frameworks as Surface Enhanced Raman Scattering Substrates with High Tailorability. Journal of the American Chemical Society, 2019, 141, 870-878.	6.6	204
12	Efficient Visible Light Active CaFe ₂ O ₄ /WO ₃ Based Composite Photocatalysts: Effect of Interfacial Modification. Journal of Physical Chemistry C, 2009, 113, 17132-17137.	1.5	178
13	Towards full-colour tunability of inorganic electrochromic devices using ultracompact fabry-perot nanocavities. Nature Communications, 2020, 11, 302.	5.8	167
14	Hierarchical BiOCl microflowers with improved visible-light-driven photocatalytic activity by Fe(III) modification. Applied Catalysis B: Environmental, 2015, 174-175, 105-112.	10.8	155
15	Flexible Lithium-Ion Fiber Battery by the Regular Stacking of Two-Dimensional Titanium Oxide Nanosheets Hybridized with Reduced Graphene Oxide. Nano Letters, 2017, 17, 3543-3549.	4.5	148
16	Molecularly Stacking Manganese Dioxide/Titanium Carbide Sheets to Produce Highly Flexible and Conductive Film Electrodes with Improved Pseudocapacitive Performances. Advanced Energy Materials, 2017, 7, 1602834.	10.2	144
17	Versatile Cutting Method for Producing Fluorescent Ultrasmall MXene Sheets. ACS Nano, 2017, 11, 11559-11565.	7.3	136
18	Unconventional Aluminum Ion Intercalation/Deintercalation for Fast Switching and Highly Stable Electrochromism. Advanced Functional Materials, 2015, 25, 5833-5839.	7.8	132

#	Article	IF	CITATIONS
19	Single crystalline zinc stannate nanoparticles for efficient photo-electrochemical devices. Chemical Communications, 2010, 46, 1529.	2.2	131
20	Electrochromic semiconductors as colorimetric SERS substrates with high reproducibility and renewability. Nature Communications, 2019, 10, 678.	5.8	131
21	A few-layered Ti ₃ C ₂ nanosheet/glass fiber composite separator as a lithium polysulphide reservoir for high-performance lithium–sulfur batteries. Journal of Materials Chemistry A, 2016, 4, 5993-5998.	5.2	130
22	Ultrathin Twoâ€Dimensional Nanostructures: Surface Defects for Morphologyâ€Driven Enhanced Semiconductor SERS. Angewandte Chemie - International Edition, 2021, 60, 5505-5511.	7.2	123
23	Coordination-controlled single-atom tungsten as a non-3d-metal oxygen reduction reaction electrocatalyst with ultrahigh mass activity. Nano Energy, 2019, 60, 394-403.	8.2	119
24	The growth of multi-walled carbon nanotubes with different morphologies on carbon fibers. Carbon, 2005, 43, 663-665.	5.4	118
25	Electrostatic-Interaction-Assisted Construction of 3D Networks of Manganese Dioxide Nanosheets for Flexible High-Performance Solid-State Asymmetric Supercapacitors. ACS Nano, 2017, 11, 7879-7888.	7.3	116
26	Fabry–Perot Cavity-Type Electrochromic Supercapacitors with Exceptionally Versatile Color Tunability. Nano Letters, 2020, 20, 1915-1922.	4.5	115
27	Trace H ₂ O ₂ â€Assisted High apacity Tungsten Oxide Electrochromic Batteries with Ultrafast Charging in Seconds. Angewandte Chemie - International Edition, 2016, 55, 7161-7165.	7.2	107
28	Eutectoid-structured WC/W2C heterostructures: A new platform for long-term alkaline hydrogen evolution reaction at low overpotentials. Nano Energy, 2020, 68, 104335.	8.2	98
29	Surface Enhanced Raman Scattering Revealed by Interfacial Charge-Transfer Transitions. Innovation(China), 2020, 1, 100051.	5.2	98
30	Enhancing the performance of quantum dots sensitized solar cell by SiO2 surface coating. Applied Physics Letters, 2010, 96, .	1.5	96
31	Field emission from AlN nanorod array. Applied Physics Letters, 2005, 86, 153104.	1.5	91
32	Moisture-Driven Power Generation for Multifunctional Flexible Sensing Systems. Nano Letters, 2019, 19, 5544-5552.	4.5	89
33	Facile and Controlled Synthesis of 3D Nanorods-Based Urchinlike and Nanosheets-Based Flowerlike Cobalt Basic Salt Nanostructures. Journal of Physical Chemistry C, 2007, 111, 3848-3852.	1.5	88
34	Tet2 loss leads to hypermutagenicity in haematopoietic stem/progenitor cells. Nature Communications, 2017, 8, 15102.	5.8	88
35	Nanocrystalline Electrodes Based on Nanoporous-Walled WO ₃ Nanotubes for Organic-Dye-Sensitized Solar Cells. Langmuir, 2011, 27, 12730-12736.	1.6	85
36	Combined Loss of Tet1 and Tet2 Promotes B Cell, but Not Myeloid Malignancies, in Mice. Cell Reports, 2015, 13, 1692-1704.	2.9	83

#	Article	IF	CITATIONS
37	Nature-inspired construction, characterization, and photocatalytic properties of single-crystalline tungsten oxide octahedra. Chemical Communications, 2010, 46, 3321.	2.2	80
38	Using Intrinsic Intracrystalline Tunnels for Nearâ€Infrared and Visibleâ€Light Selective Electrochromic Modulation. Advanced Optical Materials, 2017, 5, 1700194.	3.6	68
39	Thermal migration towards constructing W-W dual-sites for boosted alkaline hydrogen evolution reaction. Nature Communications, 2022, 13, 763.	5.8	68
40	Shape Modulation of Tungstic Acid and Tungsten Oxide Hollow Structures. Journal of Physical Chemistry C, 2009, 113, 6539-6546.	1.5	62
41	Remarkable Near-Infrared Electrochromism in Tungsten Oxide Driven by Interlayer Water-Induced Battery-to-Pseudocapacitor Transition. ACS Applied Materials & Interfaces, 2020, 12, 33917-33925.	4.0	61
42	Direct growth of carbon nanotubes on the surface of ceramic fibers. Carbon, 2005, 43, 883-886.	5.4	58
43	Tailored Remote Photochromic Coloration of in situ Synthesized CdS Quantum Dot Loaded WO ₃ Films. Advanced Functional Materials, 2010, 20, 4162-4167.	7.8	58
44	Defect engineering in semiconductor-based SERS. Chemical Science, 2022, 13, 1210-1224.	3.7	52
45	Mimicking Nature's Butterflies: Electrochromic Devices with Dualâ€ S ided Differential Colorations. Advanced Materials, 2021, 33, e2007314.	11.1	50
46	MOF-derived vertically stacked Mn ₂ 0 ₃ @C flakes for fiber-shaped zinc-ion batteries. Journal of Materials Chemistry A, 2020, 8, 24031-24039.	5.2	48
47	Aligned coaxial tungsten oxide–carbon nanotube sheet: a flexible and gradient electrochromic film. Chemical Communications, 2012, 48, 8252.	2.2	46
48	Block copolymer templated nanoporous TiO ₂ for quantum-dot-sensitized solar cells. Journal of Materials Chemistry, 2010, 20, 492-497.	6.7	45
49	Cationic two-dimensional sheets for an ultralight electrostatic polysulfide trap toward high-performance lithium-sulfur batteries. Energy Storage Materials, 2017, 9, 39-46.	9.5	37
50	Applications of CRISPR/Cas9 Technology in theÂTreatment of Lung Cancer. Trends in Molecular Medicine, 2019, 25, 1039-1049.	3.5	37
51	An environment-friendly microemulsion approach to α-FeOOH nanorods at room temperature. Materials Research Bulletin, 2006, 41, 2238-2243.	2.7	36
52	A simple and low-temperature hydrothermal route for the synthesis of tubular α-FeOOH. Materials Letters, 2007, 61, 4794-4796.	1.3	36
53	A simple solution route to controlled synthesis of ZnS submicrospheres, nanosheets and nanorods. Nanotechnology, 2006, 17, 4731-4735.	1.3	34
54	TET2 Loss Dysregulates the Behavior of Bone Marrow Mesenchymal Stromal Cells and Accelerates Tet2-Driven Myeloid Malignancy Progression. Stem Cell Reports, 2018, 10, 166-179.	2.3	34

#	Article	IF	CITATIONS
55	Vibrant Color Palettes of Electrochromic Manganese Oxide Electrodes for Colorful Znâ€lon Battery. Advanced Optical Materials, 2021, 9, 2100637.	3.6	34
56	Fabrication of TiO ₂ /WO ₃ Composite Nanofibers by Electrospinning and Photocatalystic Performance of the Resultant Fabrics. Industrial & Engineering Chemistry Research, 2016, 55, 80-85.	1.8	33
57	Macroscopic and Strong Ribbons of Functionality-Rich Metal Oxides from Highly Ordered Assembly of Unilamellar Sheets. Journal of the American Chemical Society, 2015, 137, 13200-13208.	6.6	32
58	A novel visible-light-driven photochromic material with high-reversibility: tungsten oxide-based organic–inorganic hybrid microflowers. Chemical Communications, 2009, , 2204.	2.2	29
59	Synthesis and properties of flame-retardant poly(vinyl alcohol)/pseudo-boehmite nanocomposites with high transparency and enhanced refractive index. Polymer Degradation and Stability, 2014, 99, 53-60.	2.7	29
60	In-Situ Formation of Cobalt-Phosphate Oxygen-Evolving Complex-Anchored Reduced Graphene Oxide Nanosheets for Oxygen Reduction Reaction. Scientific Reports, 2013, 3, 2263.	1.6	28
61	Populating surface-trapped electrons towards SERS enhancement of W ₁₈ O ₄₉ nanowires. Chemical Communications, 2018, 54, 6332-6335.	2.2	28
62	Photodegradable CuS SERS Probes for Intraoperative Residual Tumor Detection, Ablation, and Self-Clearance. ACS Applied Materials & amp; Interfaces, 2019, 11, 23436-23444.	4.0	28
63	HOXBLINC long non-coding RNA activation promotes leukemogenesis in NPM1-mutant acute myeloid leukemia. Nature Communications, 2021, 12, 1956.	5.8	28
64	Preparation of elastic diglycolamic-acid modified chitosan sponges and their application to recycling of rare-earth from waste phosphor powder. Carbohydrate Polymers, 2018, 190, 255-261.	5.1	27
65	Surface Wetting Behavior of a WO ₃ Electrode under Light-Irradiated or Potential-Controlled Conditions. Journal of Physical Chemistry C, 2009, 113, 10642-10646.	1.5	26
66	Rational design of galvanically replaced Pt-anchored electrospun WO3 nanofibers as efficient electrode materials for methanol oxidation. Journal of Materials Chemistry, 2012, 22, 16514.	6.7	25
67	High prevalence of hepatitis B virus infection in patients with aggressive B cell non-Hodgkin's lymphoma in China. Annals of Hematology, 2018, 97, 453-457.	0.8	25
68	Surface-Modified Two-Dimensional Titanium Carbide Sheets for Intrinsic Vibrational Signal-Retained Surface-Enhanced Raman Scattering with Ultrahigh Uniformity. ACS Applied Materials & Interfaces, 2020, 12, 23523-23531.	4.0	25
69	Surface treatment- and calcination temperature-dependent adsorption of methyl orange molecules in wastewater on self-standing alumina nanofiber films. Journal of Materials Chemistry, 2011, 21, 14984.	6.7	24
70	Novel Cigarlike TiO ₂ Nanofibers: Fabrication, Improved Mechanical, and Electrochemical Performances. ACS Applied Materials & Interfaces, 2013, 5, 2278-2282.	4.0	23
71	Designing large-plane conjugated copolymers for the high-yield sorting of semiconducting single-walled carbon nanotubes. Chemical Communications, 2013, 49, 10492.	2.2	22
72	Color-Changing Microfiber-Based Multifunctional Window Screen for Capture and Visualized Monitoring of NH ₃ . ACS Applied Materials & Interfaces, 2018, 10, 15065-15072.	4.0	22

#	Article	IF	CITATIONS
73	Tet2 Regulates Osteoclast Differentiation by Interacting with Runx1 and Maintaining Genomic 5-Hydroxymethylcytosine (5hmC). Genomics, Proteomics and Bioinformatics, 2018, 16, 172-186.	3.0	22
74	Giant two-dimensional titania sheets for constructing a flexible fiber sodium-ion battery with long-term cycling stability. Energy Storage Materials, 2020, 24, 504-511.	9.5	22
75	Electrochromic Metamaterials of Metal–Dielectric Stacks for Multicolor Displays with High Color Purity. Nano Letters, 2021, 21, 6891-6897.	4.5	22
76	Visible-Light-Driven Superhydrophilicity by Interfacial Charge Transfer between Metal Ions and Metal Oxide Nanostructures. Langmuir, 2010, 26, 796-801.	1.6	21
77	Tailoring the structure and nitrogen content of nitrogen-doped carbon nanotubes by water-assisted growth. Carbon, 2014, 69, 247-254.	5.4	21
78	Tuning Sulfur Doping for Bifunctional Electrocatalyst with Selectivity between Oxygen and Hydrogen Evolution. ACS Applied Energy Materials, 2018, 1, 5822-5829.	2.5	21
79	An aramid nanofibers-based gel polymer electrolyte with high mechanical and heat endurance for all-solid-state NIR electrochromic devices. Solar Energy Materials and Solar Cells, 2019, 200, 109952.	3.0	21
80	Stabilizing photo-induced vacancy defects in MOF matrix for high-performance SERS detection. Nano Research, 2022, 15, 5347-5354.	5.8	21
81	Quantum Effects Enter Semiconductor-Based SERS: Multiresonant MoO ₃ · <i>x</i> H ₂ O Quantum Dots Enabling Direct, Sensitive SERS Detection of Small Inorganic Molecules. Analytical Chemistry, 2022, 94, 5048-5054.	3.2	20
82	Fast preparation of ultrafine monolayered transition-metal dichalcogenide quantum dots using electrochemical shock for explosive detection. Chemical Communications, 2016, 52, 11442-11445.	2.2	19
83	Robust and Aligned Carbon Nanotube/Titania Core/Shell Films for Flexible TCOâ€Free Photoelectrodes. Small, 2013, 9, 148-155.	5.2	18
84	W ₁₈ O ₄₉ nanowire composites as novel barrier layers for Li–S batteries based on high loading of commercial micro-sized sulfur. RSC Advances, 2016, 6, 15234-15239.	1.7	18
85	Effective decontamination of 99TcO4â^'/ReO4â^' from Hanford low-activity waste by functionalized graphene oxide–chitosan sponges. Environmental Chemistry Letters, 2020, 18, 1379-1388.	8.3	18
86	Highly selective and sensitive probes for the detection of Cr(<scp>vi</scp>) in aqueous solutions using diglycolic acid-functionalized Au nanoparticles. RSC Advances, 2019, 9, 10958-10965.	1.7	17
87	Rapid Synthesis of Sub-5 nm Sized Cubic Boron Nitride Nanocrystals with High-Piezoelectric Behavior via Electrochemical Shock. Nano Letters, 2017, 17, 355-361.	4.5	16
88	Clinical characteristics of 26 patients with primary extranodal Hodgkin lymphoma. International Journal of Clinical and Experimental Pathology, 2014, 7, 5045-50.	0.5	16
89	Molecularly Coupled Twoâ€Dimensional Titanium Oxide and Carbide Sheets for Wearable and Highâ€Rate Quasiâ€Solidâ€State Rechargeable Batteries. Advanced Functional Materials, 2019, 29, 1901576.	7.8	15
90	Ultrathin Two-Dimensional Metal–Organic Framework Nanosheets with Activated Ligand-Cluster Units for Enhanced SERS. ACS Applied Materials & Interfaces, 2022, 14, 2326-2334.	4.0	14

#	Article	IF	CITATIONS
91	Trace H ₂ O ₂ â€Assisted Highâ€Capacity Tungsten Oxide Electrochromic Batteries with Ultrafast Charging in Seconds. Angewandte Chemie, 2016, 128, 7277-7281.	1.6	13
92	Toll-like receptor 4–induced inflammatory responses contribute to the tumor-associated macrophages formation and infiltration in patients with diffuse large B-cell lymphoma. Annals of Diagnostic Pathology, 2015, 19, 232-238.	0.6	12
93	Defective cuprous oxide as a selective surfaceâ€enhanced Raman scattering sensor of dye adulteration in Chinese herbal medicines. Journal of Raman Spectroscopy, 2021, 52, 1265-1274.	1.2	12
94	Light emission and degradation of single-walled carbon nanotube filament. Journal of Applied Physics, 2005, 98, 044306.	1.1	11
95	Ultrathin Twoâ€Dimensional Nanostructures: Surface Defects for Morphologyâ€Driven Enhanced Semiconductor SERS. Angewandte Chemie, 2021, 133, 5565-5571.	1.6	11
96	Electrochemical fabrication of ultrafine g-C3N4 quantum dots as a catalyst for the hydrogen evolution reaction. New Carbon Materials, 2022, 37, 392-399.	2.9	11
97	Boosting Electrocatalytic Performances of Palladium Nanoparticles by Coupling with Metallic Single-Walled Carbon Nanotubes. Chemistry of Materials, 2014, 26, 2789-2794.	3.2	10
98	Hydroxyl Group-Abundant TiO ₂ Semiconductor SERS Sensor toward Polymerization Inhibitor Sensing. Journal of Physical Chemistry C, 2020, 124, 20530-20537.	1.5	10
99	A "three-in-one―water treatment material: nitrogen-doped tungstic acid. Chemical Communications, 2013, 49, 5787.	2.2	9
100	Clinical characteristics and prognosis of multiple myeloma with bone-related extramedullary disease at diagnosis. Bioscience Reports, 2018, 38, .	1.1	9
101	Novel prognostic scoring system for diffuse large B-cell lymphoma. Oncology Letters, 2018, 15, 5325-5332.	0.8	8
102	Clinical characteristics and prognosis associated with multiple primary malignant tumors in non-Hodgkin lymphoma patients. Tumori, 2019, 105, 474-482.	0.6	8
103	A Dopant Replacementâ€Driven Molten Salt Method toward the Synthesis of Subâ€5â€nmâ€Sized Ultrathin Nanowires. Small, 2020, 16, 2001098.	5.2	8
104	A comparison between field-emission properties of three one-dimensional carbon materials. Physica B: Condensed Matter, 2007, 396, 44-48.	1.3	7
105	The Wilms' tumor gene-1 is a prognostic factor in myelodysplastic syndrome: a meta analysis. Oncotarget, 2018, 9, 16205-16212.	0.8	7
106	A lower ALC/AMC ratio is associated with poor prognosis of peripheral T-cell lymphoma-not otherwise specified. Leukemia Research, 2018, 73, 5-11.	0.4	7
107	LOW TEMPERATURE SYNTHESIS OF Mg(OH)2 NANOTUBES IN AQUEOUS SOLUTIONS OF BLOCK COPOLYMER P123. Nano, 2006, 01, 185-189.	0.5	6
108	Control of the separation order of Au(III), Pd(II), and Pt(IV) achieved by site-controllable carboxyl-functionalized diethylaminoethyl celluloses. Cellulose, 2020, 27, 10167-10181.	2.4	6

#	Article	IF	CITATIONS
109	Infrared Electrochromic Property of the Colorful Tungsten Oxide Films. Wuji Cailiao Xuebao/Journal of Inorganic Materials, 2021, 36, 485.	0.6	6
110	Symmetry-breaking triggered by atomic tungsten for largely enhanced piezoelectric response in hexagonal boron nitride. Nano Energy, 2022, 99, 107375.	8.2	6
111	Effect of geometrical parameters on the field-emission properties of single-walled carbon nanotube ropes. Journal of Materials Research, 2003, 18, 2188-2193.	1.2	5
112	Self-standing microporous films of arrayed alumina nano-fibers including Schiff base molecules: effect of the environment around the molecules on their photo-luminescence. Journal of Materials Chemistry, 2012, 22, 9738.	6.7	5
113	Flexible Quasi-Solid-State Sodium-Ion Batteries Built by Stacking Two-Dimensional Titania Sheets with Carbon Nanotube Spacers. ACS Applied Energy Materials, 2019, 2, 5707-5715.	2.5	5
114	Off-centered-symmetry-based band structure modulation of hexagonal WO ₃ . Journal of Physics Condensed Matter, 2019, 31, 355501.	0.7	5
115	Modified conditioning regimen with idarubicin followed by autologous hematopoietic stem cell transplantation for invasive B-cell non-Hodgkin's lymphoma patients. Scientific Reports, 2021, 11, 4273.	1.6	5
116	Increased MALAT1 expression predicts poor prognosis in primary gastrointestinal diffuse large B-cell lymphoma. Clinical and Experimental Medicine, 2022, 22, 183-191.	1.9	5
117	miR‑150 is a negative independent prognostic biomarker for primary gastrointestinal diffuse large B‑cell lymphoma. Oncology Letters, 2020, 19, 3487-3494.	0.8	5
118	A simple solution route to control synthesis of Fe3O4 nanomaterials at low temperature and their magnetic properties. Science in China Series B: Chemistry, 2009, 52, 916-923.	0.8	4
119	Comorbidity as an independent prognostic factor in elderly patients with peripheral T-cell lymphoma. OncoTargets and Therapy, 2016, 9, 1795.	1.0	4
120	Simple Preparation of LaPO4:Ce, Tb Phosphors by an Ionic-Liquid-Driven Supported Liquid Membrane System. International Journal of Molecular Sciences, 2019, 20, 3424.	1.8	4
121	Correlation Between Uptake of 18F-FDG During PET/CT and Ki-67 Expression in Patients Newly Diagnosed With Multiple Myeloma Having Extramedullary Involvement. Technology in Cancer Research and Treatment, 2019, 18, 153303381984906.	0.8	4
122	EVI1 expression predicts outcome in higher-risk myelodysplastic syndrome patients. Leukemia and Lymphoma, 2018, 59, 2929-2940.	0.6	3
123	Overexpression of microRNA‑130a predicts adverse prognosis of primary gastrointestinal diffuse large B‑cell lymphoma. Oncology Letters, 2020, 20, 1-1.	0.8	3
124	Characteristics of myeloid sarcoma in mice and patients with TET2 deficiency. Oncology Letters, 2020, 19, 3789-3798.	0.8	3
125	The efficiency of autologous stem cell transplantation as the first-line treatment for nodal peripheral T-cell lymphoma: results of a systematic review and meta-analysis. Expert Review of Hematology, 2022, 15, 265-272.	1.0	2
126	LOW TEMPERATURE SYNTHESIS OF Fe-DOPED ZnO NANOROD BUNDLES IN AQUEOUS SOLUTION. Nano, 2006, 01, 153-157.	0.5	1

#	Article	IF	CITATIONS
127	Shaping different carbon nano- and submicro-structures by alcohol chemical vapor deposition. Journal of Materials Research, 2006, 21, 2504-2509.	1.2	1
128	APD Compressible Aerogel-Like Monoliths with Potential Use in Environmental Remediation. Materials, 2019, 12, 3459.	1.3	1
129	Multiplex ligation-dependent probe amplification identifies copy number changes in normal and undetectable karyotype MDS patients. Annals of Hematology, 2021, 100, 2207-2214.	0.8	1
130	Fabrication of Low-Voltage Electron Source from Patterned Arrays of Aligned Single-Walled Carbon Nanotube Ropes. Japanese Journal of Applied Physics, 2005, 44, 7713-7716.	0.8	0
131	17. Electrochromic and photovoltaic applications of nanocarbon hybrids. , 2014, , 455-474.		0
132	Modified Conditioning Regimen with Idarubicin Prior to Autologous Hematopoietic Stem Cell Transplantation in B-Cell Non-Hodgkin Lymphoma. Blood, 2019, 134, 5349-5349.	0.6	0